

ORIGINAL ARTICLE

Potential of CeO₂-TiO₂ NCs for the photocatalytic degradation of antibiotics Ciprofloxacin and Levofloxacin

Harshulika Singh¹, Amit Ahlawat^{1,2}, Tarun Kumar Dhiman¹, Mrinal Poddar¹, Anees A. Ansari³,
Pratima R. Solanki^{*}

¹Special Center for Nanoscience, Jawaharlal Nehru University, New Delhi-110067

²Deenbandhu Chhotu Ram University of Science and Technology, Department of Physics, Murthal-131039

³King Abdullah Institute for Nanotechnology, King Saud University, Riyadh-11451, Saudi Arabia

* Email: partima@mail.jnu.ac.in; pratimarsolanki@gmail.com

ABSTRACT

Cerium oxide- titanium oxide hybrid nanocomposite (CeO₂-TiO₂NC) was prepared by co-precipitation process for the photocatalytic decay of the antibiotics. X-ray diffraction study shows a cubic structure with the crystallite size of 19 nm of CeO₂-TiO₂NC. UV-vis spectroscopy showed two distinct peaks (275 nm and 300 nm) corresponding to CeO₂ and TiO₂, with a band gap of 3.3 eV. Scanning electron microscope having Energy dispersive X-ray was applied to find out the morphology and chemical or elemental analysis of CeO₂-TiO₂NC that confirmed the composite formation. Raman study shows the most dominant characteristic vibrational modes of the CeO₂-TiO₂NCs at lower frequency range. The degradation of Ciprofloxacin (CIP) and Levofloxacin (LEVO) was investigated under dark, visible, and UV light irradiation under an ambient environment at neutral pH. The highest degradation of LEVO and CIP was obtained as 97.89 % and, 91.78%, respectively under UV- light irradiation with 120 minutes.

Keywords: Fluoroquinolone; Antibiotics; Ciprofloxacin; Levofloxacin and CeO₂-TiO₂nc.

Received 10.12.2023

Revised 12.02.2024

Accepted 27.04.2024

INTRODUCTION

Antibiotics are one of the top accomplishments in microbiology. They are strong therapeutic drugs for bacterial diseases (1). Recently, people have been excessively using these antibiotics which cannot be completely metabolized inside their bodies and excreted out. These antibiotics are present in wastewater and make their way to groundwater, rivers and other water sources. Even though they have a short shelf-life, this causes serious harm to humans and the ecosystem (2). They damage the ecosystem by exposing microbial community in water sources, promotes generation of antibiotic-resistant genes and bacteria, and acute to chronic toxicity for humans and other organisms (3–5).

Ciprofloxacin (CIP) and Levofloxacin (LEVO) are synthetic second-generation fluoroquinolones class antibiotic drugs. Several side effects may occur from fluoroquinolones depending on different personal or overdose which may even lead to death. CIP is used for bacterial infections such as anthrax and certain types of plague. Side effects include allergic reaction, nerve damage, tendon issues, aorta damage, low blood sugar, and jaundice. It also hinders the synthesis of protein and DNA by causing interference with the enzymes that helps DNA rewinding, killing the bacteria (6). CIP concentration in water sources even as low as 0.2% (v/v) has been reported to significant growth rate reduction for tadpoles (7). LEVO is used for bacterial infections such as chronic bronchitis, pneumonia and infections of kidney, sinus, urinary tract, eyes, skin, and prostate. Side effects include allergic reactions, liver damage, seizures, intestine infection, nerve damage, heart rhythm fluctuations, sugar level fluctuations, and photosensitivity. In environment, significant growth rate reduction in different green algae (*Chlorella vulgaris* and *Microcystis flos-aquae*) have been reported in the presence of LEVO (8,9).

Therefore, this is of utmost importance to treat wastewater before expelling it to the environment. Many different methods have been deployed for effective wastewater treatment for antibiotic removal or degradation, such as biological treatment, reverse osmosis, photocatalytic degradation, sorption techniques, membrane filtration, ion exchange, and electrocoagulation (10–19). Due to their chemical stability and non-biodegradable nature, conventional methods could not achieve optimum removal

efficiency. Whereas, photocatalytic reaction can degrade these contaminations completely into carbon dioxide, water, and mineral acids (11,20,21) using nanomaterials.

Titanium dioxide (TiO₂) has been utilized for photocatalytic degradation of several organic and inorganic contaminants in water. It has good stability, economical, excellent light adsorption, low toxicity, and easy recovery by filtration and centrifugation methods (22,23). However, it has a large band gap which restricts its adsorption to UV range only. This drawback has been taken care of using doping or forming composites with different nanoparticles (24–26). Rare earth metals and their oxides which combined with TiO₂, leads to red shift by forming inter-band states (15,27). Also, their addition reduces electron-hole pair recombination by trapping them in inter-bands and accelerating their mobility over TiO₂ surface (28,29). Cerium (Ce) has shown activity in the visible light region when combined with TiO₂ (30–32). Cerium oxide (CeO₂) is an active rare earth metal oxide, it shows excellent stability, easily accessible due to excess quantity, non-toxicity, and economical nature (33,34). It has been used in many different applications such as, pollution control, oxygen sensors, solid oxide fuel cells, hydrogen generation and wastewater treatment (16,23,35). It is reported that the nanocomposite of CeO₂-TiO₂NC exhibits the synergistic effect, resulting in an increasing photocatalytic activity by strengthening the optical absorption property. CeO₂-TiO₂NC for methyl red (36) and CeO₂-TiO₂-graphene (37) nanocomposites used for the photocatalytic degradation of pollutants and reported improved results. Besides this, CeO₂-TiO₂NC used this for degradation of bis-*p*-nitrophenyl phosphate and chemical warfare agents (38) and authors claimed the improved the degradation capability due to the synergetic effects of CeO₂-TiO₂. Thus, there is wide scope to explore the photocatalytic degradation of antibiotics using CeO₂-TiO₂NC. Table 1 shows the comparison of degradation of antibiotics using different nanomaterials.

In this context, CeO₂-TiO₂NC was synthesized using the co-precipitation method for degradation of CIP and LEVO. The chemical composition, crystal structure, and crystallinity of the CeO₂-TiO₂NC were ascertained by means of an X-ray diffraction spectroscopy (XRD) technique. The structural morphology of CeO₂-TiO₂NC was confirmed using Scanning Electron Microscopy (SEM). The chemical composition of the as-prepared CeO₂-TiO₂NC was monitored by energy dispersive X-ray analysis (EDX).

Table 1. Comparison of antibiotics degradation using nanomaterials.

S. No.	Nanoparticles	Synthesis Techniques	K value (min ⁻¹)	Degradation time (min)	Efficiency %	Reference
1	CoTiO ₃ /CeO ₂ heterostructures	Sol-gel process	0.0417	90	100 (CIP)	(39)
2	Ag ₂ CO ₃ /CeO ₂ /AgBr	hydrobromic acid corrosion	-	40	88 (LEVO)	(40)
3	Cerium oxide/MXT composite.	hybrid methodology	0.5	103	94.7 (Tetracycline)	(41)
4	CeO ₂ /Co ₃ O ₄	facile chemical reaction		50	90 (CIP)	(42)
5	AgCl/ZIF-8/C-TiO ₂	Hydrothermal	0.043	60	97.3 (CIP)	(43)
6	CeO ₂ -TiO ₂ NC	Co-precipitation	0.017 0.54	120	97.89 (LEVO) 91.78 (CIP)	This work

MATERIAL AND METHODS

Chemicals used

Titanium isopropoxide (TIP) (97%, Aldrich Chemicals), isopropanol (99%, Rankem), cerium nitrate hexahydrate (99%, Thomas Baker), and sodium hydroxide (98%, Fisher Scientific). Levofloxacin (LEVO) and Ciprofloxacin (CIP) were purchased from Sigma Aldrich of 99% purity.

2.2 Synthesis of the CeO₂-TiO₂NC

The pre-calculated amount, i.e., 5 mL TIP and 10 mL isopropanol, of precursor was mixed with DI water. The gel preparation process was started following the mixing of the solutions by vigorous stirring. Hydrolysis of TIP yielded a turbid solution that was heated at 70°C for approximately 18–20 h. The precipitated sample was then collected and washed thrice with ethanol to neutralize the sample. This precipitate was collected and dried for 24 h at 80°C. Finally, the prepared powder was annealed at 400°C for 3 h. To synthesize CeO₂ nanoparticles (NPs), Ce(NO₃)₂·6H₂O was added to 100 mL DI water to prepare a 0.25 M solution. This solution was mixed under regular stirring with the as-prepared TiO₂ NPs by using the titration method. Following the complete mixing of CeO₂ and TiO₂ NPs, the solution was stirred for some time and then dried at 80°C for 5 h. The resultant CeO₂-TiO₂nc was calcined at 500°C for 4 h.

Characterization

X-ray diffraction pattern was measured from Rigaku Miniflex, Japan. Scanning electron microscopy (SEM) and Energy dispersive x-ray (EDX) analysis was carried out to determine the chemical composition of the as-prepared NC material using JSM-IT200 JEOL, JAPAN. UV/Vis spectrophotometer was applied to examine the optical absorption and photocatalytic activities using T90 + UV/VIS Spectrometer. Raman shift was carried out in the range of 500-2000 cm^{-1} using EnSpectr R532, laser of WITEC system.

Photo-catalysis study

Solutions of LEVO and CIP (10 ppm concentration) in 30 mL of DI water were prepared for degradation studies. Next, 30 mg of $\text{CeO}_2\text{-TiO}_2\text{nc}$ was added to 30 mL of the LEVO and CIP solutions separately in two beakers. The photocatalytic study of LEVO and CIP compounds were performed under three irradiation conditions: without light, visible light ($\lambda > 400 \text{ nm}$) generated through a 100 W power bulb (Philips), and UV light ($\lambda < 400 \text{ nm}$) generated through a 300 W power bulb (Osram). The beaker was positioned 15 cm from the two bulbs. Next, 4 mL of sample was collected at regular intervals of 0, 20, 40, 60, 80, 100 and 120 min in micro centrifuge tubes. The tubes were then centrifuged (Eppendorf Centrifuge 5424R) to obtain a supernatant. UV-Vis spectra were acquired with a UV-Vis spectrometer to study the sequential degradation of LEVO and CIP compounds. The reutilization of the catalyst was investigated by the cyclic photocatalytic study. The used catalyst was centrifuged after the first degradation study to remove the adsorbed molecules. The catalyst was then washed 4–5 times using DI water. Centrifugation was performed one more time to remove the remaining adsorbed molecules. $\text{CeO}_2\text{-TiO}_2\text{nc}$ was further studied for 4 degradation cycles of LEVO and CIP.

RESULTS AND DISCUSSION

Crystallographic study

Figure 1 shows the XRD spectra of $\text{CeO}_2\text{/TiO}_2\text{nc}$ in the range of 10–80°. TiO_2 peaks are indicated by the (*) mark and are positioned at 28.32°, 35.95°, and 67.42° corresponding to (101), (004), and (204) planes, respectively. The remaining peaks in the spectra of $\text{CeO}_2\text{/TiO}_2\text{nc}$ are corresponding to CeO_2 at the positions of 31.17°, 32.95°, 47.2°, 56.13°, 59.7°, and 62.45° corresponding to (111), (200), (220), (311), (222), and (400), respectively (44). The average crystallite size was calculated using the Debye–Scherrer equation as explained in our previously published paper (44). The average crystallite size as 19 nm for $\text{CeO}_2\text{-TiO}_2\text{nc}$ was obtained. The existence of cubic CeO_2 and anatase TiO_2 phases were confirmed by XRD.

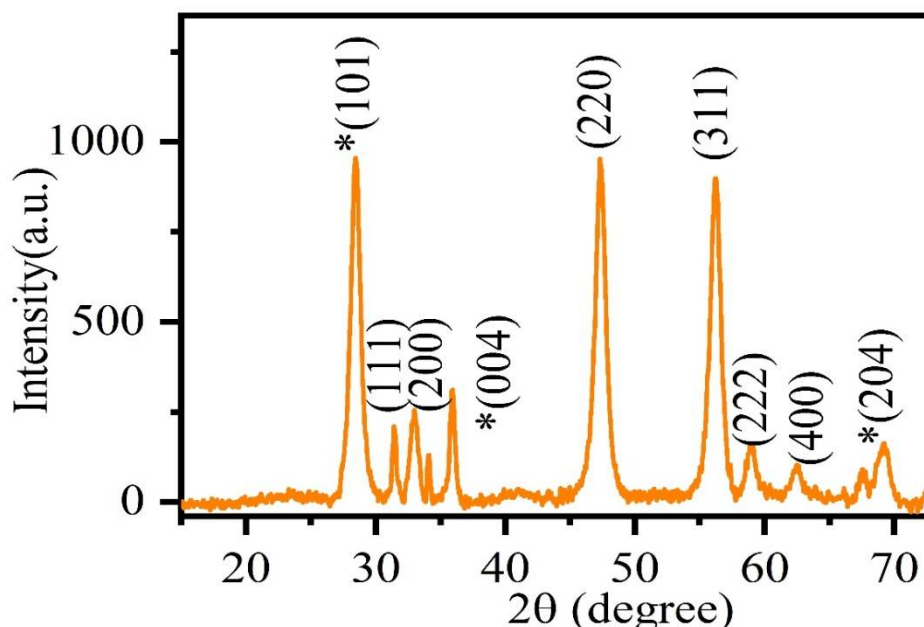


Fig. 1: XRD analysis of the $\text{CeO}_2\text{-TiO}_2\text{nc}$.

Morphological characterization

Figure 2 shows the SEM images with EDX to verify the morphological study and element distribution of $\text{CeO}_2\text{-TiO}_2\text{nc}$. EDX analysis was used to determine the chemical composition and phase purity of the $\text{CeO}_2\text{-TiO}_2\text{nc}$ NC. The mapping shows equitable distribution of the Ti, Ce and O in the $\text{CeO}_2\text{-TiO}_2\text{nc}$ results confirm that formation of $\text{CeO}_2\text{-TiO}_2\text{nc}$.

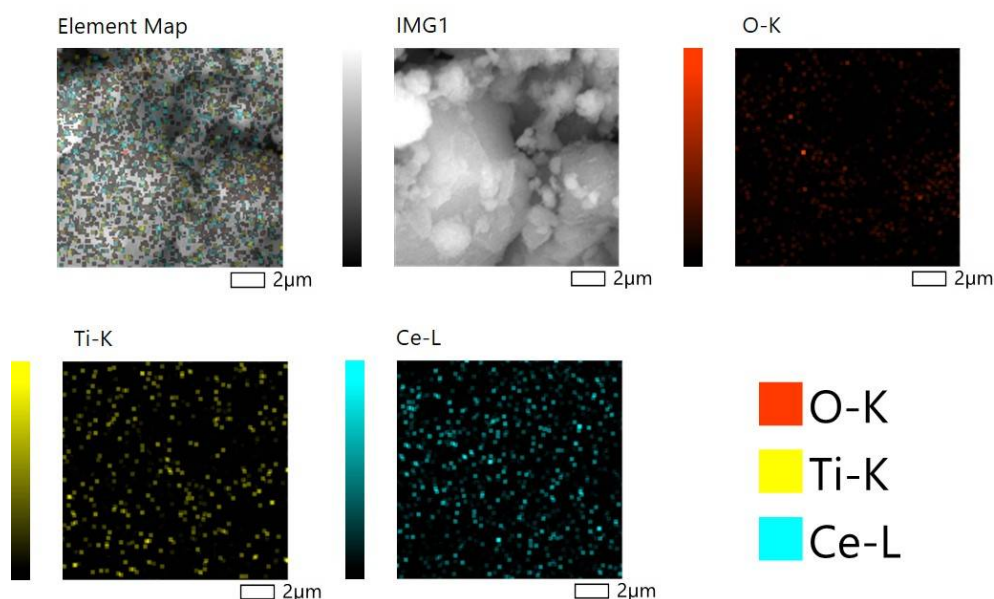


Fig. 2:

Elemental analysis of the CeO₂-TiO₂nc.

Optical absorption properties

Figure 3 shows the UV-Vis spectra of the as-prepared hybrid NC material. Two small peaks were obtained at 275 and 300 nm corresponding to TiO₂ and CeO₂, respectively. The optical band gap (E_g) was determined from the absorption profiles of CeO₂/TiO₂nc by using the Tauc plot given by

$$(\alpha h\nu)^2 = A(h\nu - E_g)$$

where α is the absorption coefficient, h is Planck's constant, ν is the frequency of incident light, A is the proportionality constant, and E_g is the optical band gap. A band gap of 3.3 eV was noted, which can allow for effective charge carrier separation and less electron-hole recombination (45) (46).

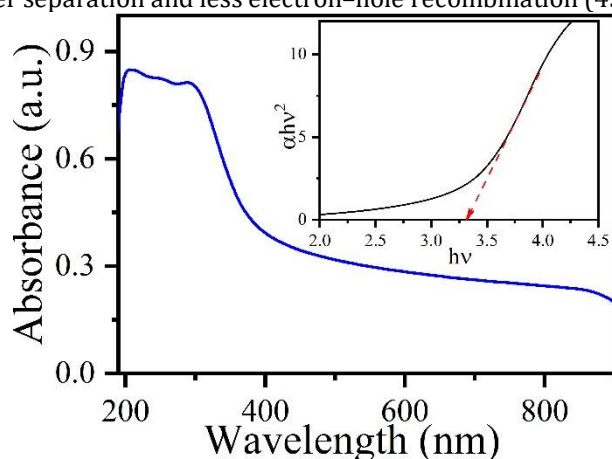


Fig. 3: UV absorption of CeO₂/TiO₂nc. The inset shows Tauc's plot

Raman shift

Figure 4 shows the Raman spectra of the CeO₂-TiO₂ NC. A prominent Raman shift is detected at 461 cm⁻¹ corresponds to the F_{2g} vibrational mode of the CeO₂. The major peak corresponding to CeO₂ have been obtained at 461 cm⁻¹ which is due to the F_{2g} mode (47,48). The peak corresponding to the TiO₂ has been obtained at three places 400, 517, and 639 cm⁻¹ corresponding to the B_{1g}, A_{1g}+B_{1g} and E_g modes of the anatase TiO₂. The Raman study confirms the formation of pure CeO₂ and TiO₂ NPs in CeO₂-TiO₂ NC (49) (50).

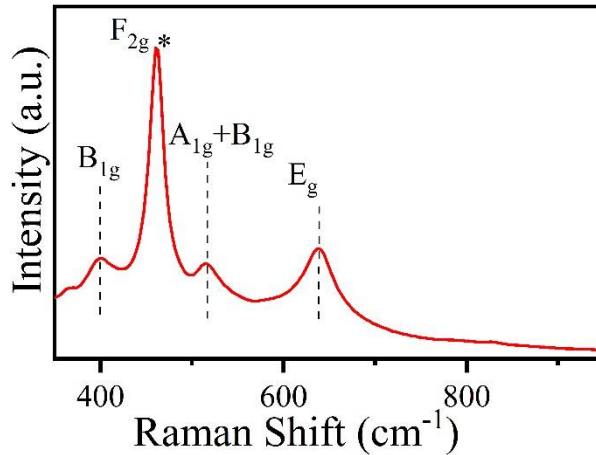


Fig. 1: Raman spectra of the CeO₂-TiO₂nc

Photocatalytic degradation of antibiotics: LEVO and CIP

Photodegradation of selected LEVO and CIP was done individually using catalyst CeO₂/TiO₂nc. It has been observed that the in dark and under visible light conditions, both LEVO and CIP showed no noticeable change in the UV-Vis absorption value. It could be due to the larger wavelength and less energy of visible light that does not cause electron excitation to promote higher photo-degradation at the surface of the nanomaterials (3,5,22). While under UV light, LEVO and CIP concentrations decreased drastically as shown in Fig. 4 and Fig. 5 (10,17). However, under UV light, more than 97.89% degradation was achieved for LEVO and over 91.78% for CIP in 120 minutes. This finding shows that the short wavelength and high energy of UV light facilitate CeO₂/TiO₂nc in the photocatalytic degradation process. The degradation percentages of LEVO and CIP were calculated using the formulae.

$$n = \frac{(C_i - C_f)}{C_i} \times 10$$

Where, c_i is the initial concentration of the antibiotics and c_f is the final concentration of the antibiotics. In both studies, UV-Vis spectroscopy was used to determine the initial and final concentrations of the antibiotics, and the peak was noted at 275 nm. The kinetics of the photocatalytic degradation of LEVO and CIP and CeO₂/TiO₂nc can be expressed as follows:

$$-\left(\frac{dC}{dt}\right) = KC$$

Where, K is the pseudo-first-order reaction rate constant, C is the concentration of antibiotics molecules at time t, and t is the reaction time. By integrating the above equation and taking the limits as $c = c_o$ at time $t = 0$, obtained here

$$\ln \ln \left(\frac{C_o}{C}\right) = Kt$$

By using the above equation, the pseudo-first-order rate constant for both the studies have been tabulated in Table 2. Rate constant (k) for LEVO and CIP was obtained as 0.017 and 0.54, respectively.

Table 2. Values of R square and K for LEVO and CIP antibiotics degradation under UV light

S. No.	Compound	R ²	k value (s ⁻¹)	Degradation %
1.	Levofloxacin	0.89	0.017	97.89
2.	Ciprofloxacin	0.88	0.54	91.78

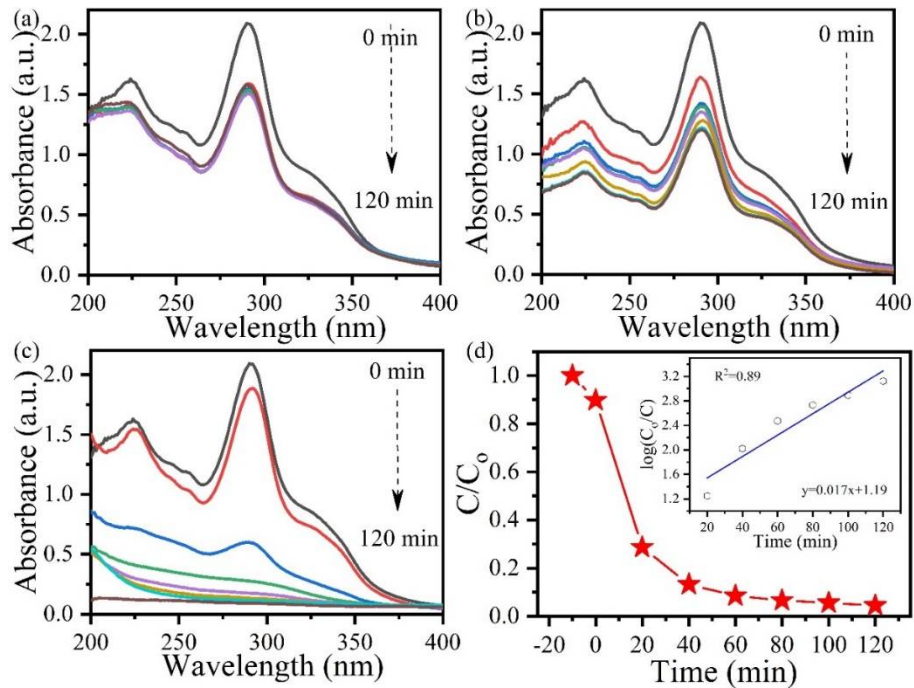


Fig. 4: The photocatalytic activity of CeO₂/TiO₂nc in (a) dark, (b) visible light, and (c) UV light; (d) C/C₀ plot of plot(c) and inset shows the pseudo-first-order reaction kinetic study for LEVO.

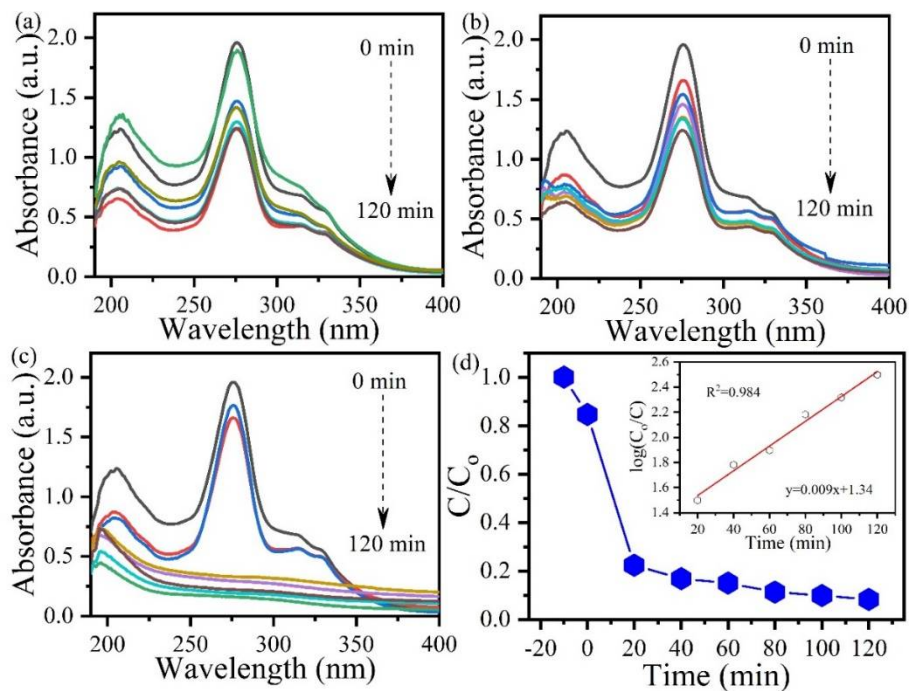


Fig. 5: The photocatalytic activity of CeO₂/TiO₂nc in (a) dark, (b) visible light, and (c) UV light; (d) C/C₀ plot of plot and inset shows the pseudo-first-order reaction kinetic study for CIP.

Cyclic Photocatalytic Study

The cyclic photo-degradation study enables determining the reutilization capacity of CeO₂/TiO₂nc for multiple reuses. As shown in Fig. 6, CeO₂/TiO₂NC was reused for three cycles of the photocatalytic study. The overall degradation percentage was >85% for LEVO and CIP after three cycles of photocatalytic study.

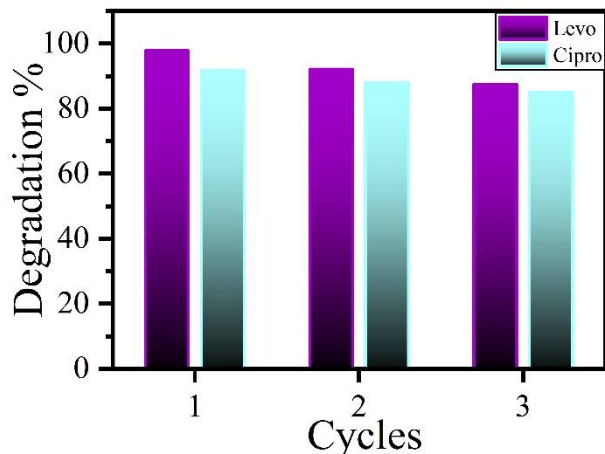


Fig. 6: Cyclic photocatalytic study of CeO₂/TiO₂NC for degrading LEVO and CIP.

Mechanism of the photo-catalytic degradation of CIP and LEVO

Figure 7 shows the mechanism of photocatalysis. Commonly, in semiconductors, electrons are excited from the valence band (VB) to the conduction band (CB) in the presence of light, which leads to a redox reaction (51). In the present case, there are different band positions because of the CB and VB of CeO₂ and TiO₂. Based on the band gap, both CeO₂ and TiO₂ are considered semiconductors. Under irradiation with UV light, both these semiconductors are excited, which leads to the production of photo-generated electrons and holes. These photo-generated electrons are excited and reach the CB, while the photo-generated holes remain at the VB. The difference in electronegativity between CeO₂ and TiO₂ leads to a transfer of electrons from the conducting materials to the surface of LEVO and CIP. On the surface of LEVO and CIP, redox reactions occur, which leads to the degradation of LEVO and CIP due to the generation of OH[•] radicals (51,52). The electrons from the CB of the nanocomposites are responsible for the reduction process, which leads to the generation of O₂⁻, and OH[•] radicals, whereas the VB leads to the oxidation process and generation of OH[•] and OH⁻ radicals, which further recombine with the functional groups of antibiotics to break them into smaller harmless compounds. The mineralization process was the dominant process for the degradation of LEVO and CIP antibiotics(44,45,53).

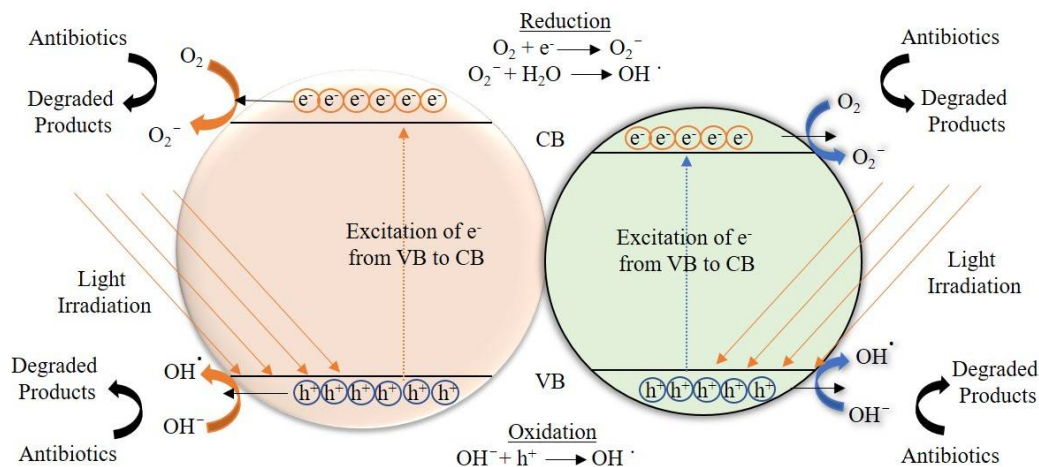


Fig. 7: Mechanism for the degradation of antibiotics using CeO₂-TiO₂nc.

CONCLUSION

CeO₂-TiO₂nc was synthesized by the co-precipitation method. The XRD study confirmed the formation of a cubic structure for CeO₂-TiO₂nc, with an average crystallite size of 19 nm. UV-vis spectroscopy showed two distinct peaks corresponding to CeO₂ and TiO₂, with a band gap of 3.3 eV. The photocatalytic study was performed under three irradiation conditions: in the dark, under visible light, and under UV light. The maximum degradation percentage for LEVO and CIP antibiotics were obtained as 97.3% and 99.8%, respectively in 120 min under UV irradiation. The degradation reaction rate constant was found as 0.017 and 0.54 for LEVO and CIP, respectively.

ACKNOWLEDGMENTS

The Government of India provides financial supports for this work [Indo-Russia project (DBT/IC-2/Indo-Russia/2017-19/02)]. The authors extend their appreciating to researchers supporting project number (RSP2023R365), King Saud University, Riyadh, Saudi Arabia.

AUTHOR CONTRIBUTION

Harshulika Singh and Tarun Kumar Dhiman: Conceptualization, Methodology, Software, Writing- Original draft preparation. Mrinal Poddar and Amit Ahlawat: Methodology, Writing - Original Draft. Anees A. Ansari and Pratima R. Solanki: Visualization, Investigation, Supervision, Writing- Reviewing and Editing.

COMPETING INTERESTS

The authors declare no competing interests.

REFERENCES

1. Qin K, Zhao Q, Yu H, Xia X, Li J, He S, et al. (2021). A review of bismuth-based photocatalysts for antibiotic degradation: Insight into the photocatalytic degradation performance, pathways and relevant mechanisms. *Environ Res.* 199:111360.
2. Trojanowicz M. Removal of persistent organic pollutants (POPs) from waters and wastewaters by the use of ionizing radiation. *Sci Total Environ.* 2020;718:134425.
3. Meredith HR, Srimani JK, Lee AJ, Lopatkin AJ, You L. Collective antibiotic tolerance: mechanisms, dynamics and intervention. *Nat Chem Biol.* 2015;11(3):182–8.
4. Berendonk TU, Manaia CM, Merlin C, Fatta-Kassinos D, Cytryn E, Walsh F, et al. Tackling antibiotic resistance: the environmental framework. *Nat Rev Microbiol.* 2015;13(5):310–7.
5. Sharma VK, Johnson N, Cizmas L, McDonald TJ, Kim H. A review of the influence of treatment strategies on antibiotic resistant bacteria and antibiotic resistance genes. *Chemosphere.* 2016;150:702–14.
6. Giri AS, Golder AK. Ciprofloxacin degradation from aqueous solution by Fenton oxidation: reaction kinetics and degradation mechanisms. *Rsc Adv.* 2014;4(13):6738–45.
7. Gunnarsson L, Kristiansson E, Rutgersson C, Sturve J, Fick J, Förllin L, et al. Pharmaceutical industry effluent diluted 1: 500 affects global gene expression, cytochrome P450 1A activity, and plasma phosphate in fish. *Environ Toxicol Chem.* 2009;28(12):2639–47.
8. Xiong JQ, Kurade MB, Jeon BH. Biodegradation of levofloxacin by an acclimated freshwater microalga, *Chlorella vulgaris*. *Chem Eng J.* 2017;313:1251–7.
9. Wan J, Guo P, Zhang S. Response of the cyanobacterium *Microcystis flos-aquae* to levofloxacin. *Environ Sci Pollut Res.* 2014;21:3858–65.
10. Chen J, Liu YS, Zhang JN, Yang YQ, Hu LX, Yang YY, et al. Removal of antibiotics from piggery wastewater by biological aerated filter system: treatment efficiency and biodegradation kinetics. *Bioresour Technol.* 2017;238:70–7.
11. Olusegun SJ, Larrea G, Osial M, Jackowska K, Krysinski P. Photocatalytic degradation of antibiotics by superparamagnetic iron oxide nanoparticles. Tetracycline case. *Catalysts.* 2021;11(10):1243.
12. Liang C, Wei D, Zhang S, Ren Q, Shi J, Liu L. Removal of antibiotic resistance genes from swine wastewater by membrane filtration treatment. *Ecotoxicol Environ Saf.* 2021;210:111885.
13. Hou J, Chen Z, Gao J, Xie Y, Li L, Qin S, et al. Simultaneous removal of antibiotics and antibiotic resistance genes from pharmaceutical wastewater using the combinations of up-flow anaerobic sludge bed, anoxic-oxic tank, and advanced oxidation technologies. *Water Res.* 2019;159:511–20.
14. Baran W, Adamek E, Jajko M, Sobczak A. Removal of veterinary antibiotics from wastewater by electrocoagulation. *Chemosphere.* 2018;194:381–9.
15. Li Q, Bao X, Sun J, Cai S, Xie Y, Liu Y, et al. Fabrication of superhydrophobic composite coating of hydroxyapatite/stearic acid on magnesium alloy and its corrosion resistance, antibacterial adhesion. *J Mater Sci.* 2021;56:5233–49.
16. Sharma M, Poddar M, Gupta Y, Nigam S, Avasthi DK, Adelung R, et al. Solar light assisted degradation of dyes and adsorption of heavy metal ions from water by CuO–ZnO tetrapodal hybrid nanocomposite. *Mater Today Chem.* 2020;17:100336.
17. Alonso JJS, El Kori N, Melián-Martel N, Del Río-Gamero B. Removal of ciprofloxacin from seawater by reverse osmosis. *J Environ Manage.* 2018;217:337–45.
18. Alnajrani MN, Alsager OA. Removal of antibiotics from water by polymer of intrinsic microporosity: Isotherms, kinetics, thermodynamics, and adsorption mechanism. *Sci Rep.* 2020;10(1):794.
19. Nagamine M, Osial M, Jackowska K, Krysinski P, Widera-Kalinowska J. Tetracycline photocatalytic degradation under CdS treatment. *J Mar Sci Eng.* 2020;8(7):483.
20. Bagheri S, TermehYousefi A, Do TO. Photocatalytic pathway toward degradation of environmental pharmaceutical pollutants: structure, kinetics and mechanism approach. *Catal Sci Technol.* 2017;7(20):4548–69.
21. Olusegun SJ, de Sousa Lima LF, Mohallem NDS. Enhancement of adsorption capacity of clay through spray drying and surface modification process for wastewater treatment. *Chem Eng J.* 2018;334:1719–28.
22. Kansal SK, Kundu P, Sood S, Lamba R, Umar A, Mehta SK. Photocatalytic degradation of the antibiotic levofloxacin using highly crystalline TiO₂ nanoparticles. *New J Chem.* 2014;38(7):3220–6.

23. Magesh G, Viswanathan B, Viswanath RP, Varadarajan TK. Photocatalytic behavior of CeO₂-TiO₂ system for the degradation of methylene blue. 2009;
24. Bessekhoud Y, Chaoui N, Trzpit M, Ghazzal N, Robert D, Weber J V. UV-vis versus visible degradation of Acid Orange II in a coupled CdS/TiO₂ semiconductors suspension. *J Photochem Photobiol A Chem.* 2006;183(1-2):218-24.
25. Wu L, Jimmy CY, Fu X. Characterization and photocatalytic mechanism of nanosized CdS coupled TiO₂ nanocrystals under visible light irradiation. *J Mol Catal A Chem.* 2006;244(1-2):25-32.
26. Ho W, Jimmy CY. Sonochemical synthesis and visible light photocatalytic behavior of CdSe and CdSe/TiO₂ nanoparticles. *J Mol Catal A Chem.* 2006;247(1-2):268-74.
27. Li FB, Li XZ, Cheah KW. Photocatalytic activity of neodymium ion doped TiO₂ for 2-mercaptobenzothiazole degradation under visible light irradiation. *Environ Chem.* 2005;2(2):130-7.
28. Pavasupree S, Suzuki Y, Pivsa-Art S, Yoshikawa S. Preparation and characterization of mesoporous TiO₂-CeO₂ nanopowders respond to visible wavelength. *J Solid State Chem.* 2005;178(1):128-34.
29. Tong T, Zhang J, Tian B, Chen F, He D, Anpo M. Preparation of Ce-TiO₂ catalysts by controlled hydrolysis of titanium alkoxide based on esterification reaction and study on its photocatalytic activity. *J Colloid Interface Sci.* 2007;315(1):382-8.
30. Zhang G, Ao J, Guo Y, Zhang Z, Shao M, Wang L, et al. Green synthesis and catalytic performance of nanoscale CeO₂ sheets. 2014;
31. Liu B, Zhao X, Zhang N, Zhao Q, He X, Feng J. Photocatalytic mechanism of TiO₂-CeO₂ films prepared by magnetron sputtering under UV and visible light. *Surf Sci.* 2005;595(1-3):203-11.
32. Ma Y, Bian Y, Liu Y, Zhu A, Wu H, Cui H, et al. Construction of Z-scheme system for enhanced photocatalytic H₂ evolution based on CdS quantum dots/CeO₂ nanorods heterojunction. *ACS Sustain Chem Eng.* 2018;6(2):2552-62.
33. Haneda M, Kaneko T, Kamiuchi N, Ozawa M. Improved three-way catalytic activity of bimetallic Ir-Rh catalysts supported on CeO₂-ZrO₂. *Catal Sci Technol.* 2015;5(3):1792-800.
34. Vindigni F, Manzoli M, Tabakova T, Idakiev V, Boccuzzi F, Chiorino A. Effect of ceria structural properties on the catalytic activity of Au-CeO₂ catalysts for WGS reaction. *Phys Chem Chem Phys.* 2013;15(32):13400-8.
35. Liu M, Wang S, Chen T, Yuan C, Zhou Y, Wang S, et al. Performance of the nano-structured Cu-Ni (alloy)-CeO₂ anode for solid oxide fuel cells. *J Power Sources.* 2015;274:730-5.
36. Mane CB, Khobare R V, Patil RP, Pawar RP. Photocatalytic degradation of methyl red using CeO₂, TiO₂ and CeO₂-TiO₂ nanocomposite. *Int J Appl Eng Res.* 2018;13:14372-7.
37. Ghasemi S, Setayesh SR, Habibi-Yangjeh A, Hormozi-Nezhad MR, Gholami MR. Assembly of CeO₂-TiO₂ nanoparticles prepared in room temperature ionic liquid on graphene nanosheets for photocatalytic degradation of pollutants. *J Hazard Mater.* 2012;199:170-8.
38. Henych J, Šťastný M, Němečková Z, Mazanec K, Tolasz J, Kormunda M, et al. Bifunctional TiO₂/CeO₂ reactive adsorbent/photocatalyst for degradation of bis-p-nitrophenyl phosphate and CWAs. *Chem Eng J.* 2021;414:128822.
39. Alsolami ES, Mkhali IA, Shawky A, Hussein MA. Efficient visible-light photooxidation of ciprofloxacin antibiotic over CoTiO₃-impregnated 2D CeO₂ nanocomposites synthesized by a sol-gel-based process. *Mater Sci Semicond Process* [Internet]. 2023;162:107487. Available from: <https://www.sciencedirect.com/science/article/pii/S1369800123001804>
40. Wen XJ, Niu CG, Guo H, Zhang L, Liang C, Zeng GM. Photocatalytic degradation of levofloxacin by ternary Ag₂CO₃/CeO₂/AgBr photocatalyst under visible-light irradiation: Degradation pathways, mineralization ability, and an accelerated interfacial charge transfer process study. *J Catal* [Internet]. 2018;358:211-23. Available from: <https://www.sciencedirect.com/science/article/pii/S0021951717304426>
41. Du X, Ye L, Zhu J, Ye Y, Wang A, Zhang H, et al. Novel Cerium (IV) Oxide -Ti₃C₂- titanium dioxide heterostructure photocatalyst for pharmaceutical pollutants removal: Photocatalyst characterization, process optimization and transformation pathways. *Surfaces and Interfaces* [Internet]. 2024;46:103892. Available from: <https://www.sciencedirect.com/science/article/pii/S2468023024000518>
42. Shen CH, Wen XJ, Fei ZH, Liu ZT, Mu QM. (2020). Visible-light-driven activation of peroxydisulfate for accelerating ciprofloxacin degradation using CeO₂/Co₃O₄ p-n heterojunction photocatalysts. *Chem Eng J* [Internet]. ;391:123612. Available from: <https://www.sciencedirect.com/science/article/pii/S138589471933027X>
43. Ali FD, Ammar SH, Ali ND, Abdulmajeed YR, Jabbar ZH. (2024). Synthesis of AgCl/ZIF-8/C-TiO₂ heterojunction photocatalysts for enhanced degradation of levofloxacin under visible-light. *Mater Sci Semicond Process* [Internet].172:108100. Available from: <https://www.sciencedirect.com/science/article/pii/S136980012300793X>
44. Ahlawat A, Dhiman TK, Solanki PR, Rana PS. (2022). Enhanced photocatalytic degradation of p-nitrophenol and phenol red through synergistic effects of a CeO₂-TiO₂ nanocomposite. *Catal Res.* 2(4):1-13.
45. Ahlawat A, Rana PS, Solanki PR. Studies of photocatalytic and optoelectronic properties of microwave synthesized and polyethyleneimine stabilized carbon quantum dots. *Mater Lett.* 2021;305:130830.
46. Singh AK, Ahlawat A, Dhiman TK, Lakshmi G, Solanki PR. (2021). Degradation of methyl parathion using manganese oxide (MnO₂) nanoparticles through photocatalysis. *SPAST Abstr.* 1(01).
47. Dhiman TK, Lakshmi G, Dave K, Roychoudhury A, Dalal N, Jha SK, et al. (2021). Rapid and label-free electrochemical detection of fumonisin-B1 using microfluidic biosensing platform based on Ag-CeO₂ nanocomposite. *J Electrochem Soc.*168(7):77510.
48. Dhiman TK, Lakshmi G, Roychoudhury A, Jha SK, Solanki PR. (2019). Ceria-nanoparticles-based microfluidic

- nanobiochip electrochemical sensor for the detection of ochratoxin-A. *ChemistrySelect*. 4(17):4867–73.
49. Poddar M, Lakshmi G, Sharma M, Chaudhary N, Nigam S, Joshi M, et al. (2022). Environmental friendly Polyacrylonitrile nanofiber mats encapsulated and coated with green algae mediated Titanium oxide nanoparticles for efficient oil spill adsorption. *Mar Pollut Bull*. 182:113971.
 50. Singh I, Birajdar B. (2019). Effective La-Na Co-doped TiO₂ nano-particles for dye adsorption: Synthesis, characterization and study on adsorption kinetics. *Nanomaterials*. ;9(3):400.
 51. Singh H, Ahlawat A, Dhiman TK, Solanki PR. (2023). Photocatalytic degradation of gentamicin using TiO₂ nanoparticle driven by UV light irradiation. *Mater Lett [Internet]*. 346:134504. Available from: <https://www.sciencedirect.com/science/article/pii/S0167577X23006894>
 52. Ahlawat A, Rana PS, Solanki PR. (2023). A simple and highly efficient approach towards the degradation of methylene blue and study the impact of degraded water on seed germination of cicer arietinum. *Nano Express*. 5(1):15027.
 53. Ahlawat A, Dhiman TK, Solanki PR, Rana PS. (2023). Facile synthesis of carbon dots via pyrolysis and their application in photocatalytic degradation of rhodamine B (RhB). *Environ Sci Pollut Res*. 1–8.

CITE THIS ARTICLE

Harshulika S, Amit A, Tarun KD, Mrinal P, Anees A. A, Pratima R. S. Potential of CeO₂-TiO₂ NCs for the photocatalytic degradation of antibiotics Ciprofloxacin and Levofloxacin. *Res. J. Chem. Env. Sci*. Vol 12 [2] April 2024. 01-10